

# Secretion of the Notch-1 A $\beta$ -like Peptide during Notch Signaling\*

Received for publication, December 13, 2005, and in revised form, January 23, 2006. Published, JBC Papers in Press, January 23, 2006, DOI 10.1074/jbc.M513250200

Masayasu Okochi<sup>1</sup>, Akio Fukumori<sup>1</sup>, Jingwei Jiang<sup>2</sup>, Naohiro Itoh<sup>2,5</sup>, Ryo Kimura<sup>2</sup>, Harald Steiner<sup>3</sup>, Christian Haass<sup>4</sup>, Shinji Tagami<sup>1</sup>, and Masatoshi Takeda<sup>1</sup>

From the <sup>1</sup>Department of Post-Genomics and Diseases, Division of Psychiatry and Behavioral Proteomics, Osaka University Graduate School of Medicine, Osaka 565-0871, Japan, <sup>2</sup>Discovery Research Laboratories, Shionogi and Co., Ltd., Shiga 520-3423, Japan, and <sup>3</sup>Adolf Butenandt Institute, Department of Biochemistry, Laboratory for Alzheimer and Parkinson's Disease Research, Ludwig-Maximilians University, D-80336 Munich, Germany

The canonical pathway of Notch signaling is mediated by regulated intramembrane proteolysis (RIP). In the pathway, ligand binding results in sequential proteolysis of the Notch receptor, and presenilin (PS)-dependent intramembrane proteolysis at the interface between the membrane and cytosol liberates the Notch-1 intracellular domain (NICD), a transcription modifier. Because the degradation of the Notch-1 transmembrane domain is thought to require an additional cleavage near the middle of the transmembrane domain, extracellular small peptides (Notch-1 A $\beta$ -like peptide (N $\beta$ )) should be produced. Here we showed that N $\beta$  species are indeed secreted during the process of Notch signaling. We identified mainly two distinct molecular species of novel N $\beta$ , N $\beta$ 21 and C-terminally elongated N $\beta$ 25, which were produced in an ~5:1 ratio. This process is reminiscent of the production of Alzheimer disease-associated A $\beta$ . PS pathogenic mutants increased the production of the longer species of A $\beta$  (A $\beta$ 42) from  $\beta$ -amyloid protein precursor. We revealed that several Alzheimer disease mutants also cause a parallel increase in the secretion of the longer form of N $\beta$ . Strikingly, chemicals that modify the A $\beta$ 42 level caused parallel changes in the N $\beta$ 25 level. These results demonstrated that the characteristics of C-terminal elongation of N $\beta$  and A $\beta$  are almost identical. In addition, because many other type 1 membrane-bound receptors release intracellular domains by PS-dependent intramembrane proteolysis, we suspect that the release of A $\beta$ - or N $\beta$ -like peptides is a common feature of the proteolysis during RIP signaling. We anticipate that this study will open the door to searches for markers of RIP signaling and surrogate markers for A $\beta$ 42 production.

Notch signaling is involved in cell differentiation as well as neurodegeneration (1). The canonical pathway for Notch signaling is mediated by regulated intramembrane proteolysis (RIP)<sup>2</sup> (2). In classical signaling,

ligand binding to receptors induces downstream intracellular signals, such as Ca<sup>2+</sup> influx and protein tyrosine phosphorylation. However, RIP signaling is distinct; the receptor is cleaved, liberating an intracellular fragment from the membrane that translocates to the nucleus where it modifies the transcription of target genes (3, 4).

In general, because both the ligand and the receptor for Notch signaling are transmembrane proteins, and signaling occurs only between neighboring cells, a process also called "local cell signaling" (5–7). Thus, although connections between Notch signaling and tumorigenesis have been reported (8, 9), studies to identify secreted molecules that reflect the level of Notch signaling have not been carried out. As a result, the only widely used method for measuring Notch signaling in living cells has been to employ intracellular reporter plasmids (10, 11).

Upon synthesis, the Notch-1 receptor undergoes furin-like cleavage at site (S) 1, forming a heterodimer that is expressed on the plasma membrane with the cleaved fragments (12, 13). The binding of ligands, such as DSL family proteins, at the plasma membrane induces endoproteolysis of Notch-1 by the ADAM/TACE/Kuzbanian family (14–16). This cleavage occurs at S2 within the extracellular juxtamembrane region and results in shedding of the heterodimerized Notch receptor (14–16). The resulting transmembrane fragment, referred to as Notch extracellular truncation, undergoes constitutive presenilin (PS)-dependent intramembrane proteolysis at S3 and S4, which we refer to as "dual-intramembrane proteolysis" (17–19). The S3 cleavage occurs at the interface between the membrane and cytosol, thus determining the N terminus of NICD (17, 18). The presence of the S4 cleavage near the middle of the transmembrane domain (19, 20) and FLAG-tagged N $\beta$  (19) suggests that a putative Notch-1 fragment (N $\beta$ ) is produced during the sequential proteolysis of Notch receptors. However, amino acid sequences of these Notch peptides and the composition of their molecular species remain unknown. Moreover, whether they are secreted during Notch signaling has not been determined.

Like Notch receptors,  $\beta$ -amyloid protein precursor (BAPP) undergoes PS-dependent "dual-intramembrane proteolysis" at  $\gamma$  and  $\epsilon$  sites (21).  $\gamma$ -Cleavage, which corresponds to S4 cleavage in Notch-1, results in the secretion of Alzheimer disease (AD)-associated A $\beta$  (22), whereas  $\epsilon$ -cleavage, corresponding to the S3 cleavage site in Notch-1, releases the BAPP intracellular domain, which has been suggested to regulate transcription

\* This work was supported by the "Program for the Promotion of Fundamental Studies in Health Sciences of the National Institute of Biomedical Innovation (05–26)", grants-in-aid for scientific research on priority areas "Advanced Brain Science Project," KAKENHI from the Ministry of Education, Culture, Sports, Science, and Technology, and grants-in-aid from the Japanese Ministry of Health, Labor and Welfare in Japan. The costs of publication of this article were defrayed in part by the payment of page charges. This article must therefore be hereby marked "advertisement" in accordance with 18 U.S.C. Section 1734 solely to indicate this fact.

<sup>1</sup> The on-line version of this article (available at <http://www.jbc.org>) contains supplemental Figs. S1–S3, supplemental Tables S1, and supplemental Refs. S1 and S2.

<sup>2</sup> To whom correspondence should be addressed. Dept. of Post-Genomics and Diseases, Division of Psychiatry and Behavioral Proteomics, Osaka University Graduate School of Medicine, D3, 2-2 Yamadaoka, Suita 565-0871, Japan. Tel.: 81-6-6879-3053; Fax: 81-6-6879-3059; E-mail: mokochi@psy.med.osaka-u.ac.jp.

<sup>3</sup> The abbreviations used are: RIP, regulated intramembrane proteolysis; A $\beta$ , amyloid- $\beta$  peptide; AD, Alzheimer disease; BAPP,  $\beta$ -amyloid protein precursor; HFIP,

1,1,1,3,3,3-hexamethyl-2-propanol; NICD, Notch-1 Lin/Notch Repeat CC > SS; NSAIDs, nonsteroidal anti-inflammatory drugs; N $\beta$ , Notch-1 intracellular cytoplasmic domain; MS, mass spectroscopy; MALDI-TOF, matrix-assisted laser desorption ionization; WT, wild type; N $\beta$ , Notch-1 A $\beta$ -like peptide; PS, presenilin; Tricine, N-[2-(4-aminobutyryl)-1-methyl-4-phenylbutyl]glycine; C11cine, N,N-bis[2-hydroxyethyl]glycine; CW, compound W; PMA, phorbol 12-myristate 13-acetate; CHO, Chinese hamster ovary; DAPT, N-[N-(3,5-difluorophenacetyl)-L-alanyl]-S-phosphorylglycine t-butyl ester.

(21, 23, 24). In PS-dependent proteolysis, there is some diversity in the specific sites of cleavage (19, 22, 25).<sup>3</sup> This is an important aspect of PS-dependent proteolysis because the pathological molecule A $\beta$ 42 is generated by cleavage of  $\beta$ APP at  $\gamma$ 42, a variant of the  $\gamma$ -cleavage site (22). Generally, A $\beta$ 42 accounts for ~10% of A $\beta$  production, and most familial AD-associated PS1/2 or  $\beta$ APP mutants show an increase in A $\beta$ 42 production, a peptide that plays a causative role in AD pathology (22). Although A $\beta$ 42 induces the formation of senile plaque both in familial and sporadic AD brains, the high degree of A $\beta$ 42 aggregation makes it difficult to determine whether A $\beta$ 42 generation is enhanced in the pathogenesis of sporadic AD. Therefore, a surrogate marker that precisely reflects the level of A $\beta$ 42 generation could be useful.

Elucidation of the mechanism of A $\beta$ 42 generation, i.e. how the  $\gamma$ -cleavage diversity occurs, is essential because a small change in the precision of  $\gamma$ -cleavage is sufficient to lead to AD pathology. PS-mediated intramembrane proteolysis is known to occur in many other type I transmembrane receptors at a site near the cytosolic interface of the transmembrane domains, corresponding to S3/ $\gamma$  cleavage (26, 27). Also, cleavage corresponding to the S4/ $\gamma$  site, which lies in the middle of the transmembrane domain, has been proposed for Notch-1,  $\beta$ APP, and CD44 (19, 28). Therefore, whether  $\gamma$ -like cleavage occurs in all the substrates or whether there is any diversity among cleavage sites remains unknown. Also, certain chemicals, such as some nonsteroidal anti-inflammatory drugs (NSAIDs), affect the precision of  $\gamma$ -cleavage, increasing or decreasing the generation of A $\beta$ 42 (29, 30), but whether this effect is specific to  $\beta$ APP or is shared by other substrates has not been determined.

To investigate the mechanism of N $\beta$  secretion during Notch signaling, we utilized mouse Notch-1 and its derivatives as substrates. We found that upon ligand binding full-length Notch-1 undergoes endo-proteolysis, which transmits Notch signaling and simultaneously secretes untagged N $\beta$  species. These N $\beta$  species shared a common N terminus (derived from S2 cleavage) but had distinct C termini (derived from S4 cleavage). Interestingly, in many cases, when the relative level of pathological A $\beta$ 42 was altered by expression of PS mutants or addition of certain chemicals, the relative level of N $\beta$ 25, a major species of longer N $\beta$ , changed concomitantly. These results suggested that N $\beta$  is secreted during Notch signaling and that the proteolytic processes determining the C termini of N $\beta$  and A $\beta$  are very similar.

## EXPERIMENTAL PROCEDURES

**Antibodies and Reagents**—The polyclonal antibody 6521 and the rat monoclonal antibody 5E9 were raised against a synthetic peptide (VKSEPVPEPLPSQ) corresponding to the N terminus of Notch extracellular truncation using methods described previously (31). Antibodies 9E10 against the c-Myc epitope, 4G8 against the A $\beta$  peptide, and H114 against the C terminus of Jagged-1 were purchased. Synthetic peptides VKSEPVPEPLPSQLHLMYVAA (N $\beta$ 21) and VKSEPVPEPLPSQLHL-MYVAAAFAV (N $\beta$ 25) were dissolved in Me<sub>2</sub>SO or HFIP and stored at -80 °C (32). Upon use, the peptides in HFIP were dried using a Speed-Vac and dissolved in the appropriate solution. S2474 was synthesized by Shionogi and Co. Ltd. The  $\gamma$ -secretase inhibitors (L685,458 and DAPT), PMA, NSAIDs (sulindac sulfide, indometacin, and naproxen), fenofibrate, farnesyl pyrophosphate ammonium salt, geranylgeranyl pyrophosphate ammonium salt, and Compound W (CW), 3,5-bis-(4-nitro-phenoxy)benzoic acid were purchased.

**cDNA Constructs**—The pCS2 vector containing the cDNA for mouse Jagged-1 (kind gift from Dr. Rafael Kopan) (33) and the pTracerCMV

containing in the mNotch-1 cDNA were described previously (kind gift from Dr. Jeffrey S. Nye) (34). The cDNAs encoding N1CS (mN1 LNR CC > SS) (kind gift from Dr. Rafael Kopan) (14) and Notch-1, in which the C-terminal 348 residues were replaced with a hexameric Myc tag (17), were cloned into the pcDNA3-hygro(+) vector. *HES-1-luc* (kind gift from Dr. Alain Israel) (10) and pGα981-6 constructs (kind gift from Dr. Georg W. Bornkamm) (11), which contain the firefly luciferase cDNA under control of the *HES-1* promoter and the hexamerized 50-bp EBN12-response element of the *TP-1* promoter, respectively, were described previously. The pRL-TK construct was obtained from Promega.

**Cell Culture and Cell Lines**—HEK293 cells stably expressing  $\beta$ APP sw and either WT or mutant PS1 were generated and cultured (19, 35). CHO cells stably expressing either WT PS1 or PS1 M146L were cultured as described previously (kind gift from Dr. Dennis J. Selkoe) (36). Cells stably expressing  $\beta$ APP sw, PS derivatives, or both were maintained in media supplemented with 200  $\mu$ g/ml G418, 200  $\mu$ g/ml Zeocin, or both. Cells stably expressing Jagged-1, Notch-1, or N1CS were selected with 100  $\mu$ g/ml hygromycin.

**cDNA Transfection and Reporter Assay**—To investigate the formation and function of N $\beta$ , we stably transfected HeLa, CHO, or HEK293 cells with Jagged-1, N1CS, and Notch-1 cDNA constructs using Lipofectamine 2000 (Invitrogen). To study the release of N $\beta$  during Notch signaling, HeLa or K293 cells in 8-cm dishes were transiently transfected with 5  $\mu$ g of plasmids encoding Notch ligands and/or receptors, 5  $\mu$ g of plasmids encoding the firefly luciferase reporter (*HES-1-luc* or pGα981-6), and 50 ng of the control *Renilla* luciferase reporter plasmid pRL-TK. The next day, the media were replaced, and the cells were lysed with 1× Passive Lysis Buffer (500  $\mu$ l) (Promega) and freeze-thaw treatment. The pulse-chase experiment to detect the N $\beta$  level was carried out at the same time. Firefly and *Renilla* luciferase activities in the lysates were measured with a dual luciferase reporter assay system (Promega).

**Pulse-Chase Experiment**—The cells were treated for 2 h with 1  $\mu$ M L685,458 or 1  $\mu$ M DAPT to inhibit  $\gamma$ -secretase activity or 20 ng/ml PMA to increase the efficiency of S2 cleavage. Next, following starvation in methionine-free minimum Eagle's medium, the cells were metabolically labeled overnight with 450  $\mu$ Ci of [<sup>35</sup>S]methionine/cysteine (Redivue Promix; Amersham Biosciences) containing 5% dialyzed (i.e. amino acid-free) fetal calf serum and  $\gamma$ -secretase inhibitors or PMA. NSAIDs, compound W, fenofibrate, farnesyl pyrophosphate ammonium salt, and geranylgeranyl pyrophosphate ammonium salt were added to the media throughout the pulse periods.

**Immunoprecipitation/Immunoblotting or Immunoprecipitation/Immunoradiography**—Collected conditioned media were adjusted to 50 mM Tris (from a stock solution of 1 M Tris, pH 7.4), 1:1000 protease inhibitor mixture (Sigma), and 5 mM EDTA (from a stock solution of 500 mM EDTA, pH 8.0). Next, the media were subjected to immunoprecipitation with antibodies 6521 or 4G8 for N $\beta$  and A $\beta$ , respectively (19). For Jagged-1 and Notch-1 derivatives, cell lysates were prepared (37) and analyzed by immunoprecipitation with antibodies H114 and 9E10, respectively (19). Proteins were separated by Tris-glycine (Invitrogen), Tris-Tricine (Invitrogen), or Tris-Bicinchoninic Acid (BCA) SDS-PAGE as described previously (38). The gels were fixed in 50% methanol, 10% acetic acid or 50% methanol, 5% glutaraldehyde (for N $\beta$ ). For immunoblotting, proteins were electrophoretically transferred to a polyvinylidene difluoride membrane and probed with the indicated antibodies (39). For autoradiography, the gels were dried and analyzed by fluorography (19).

<sup>3</sup> S. Tagami, A. Fukumori, and M. Okochi, manuscript in preparation.



**Immunoprecipitation/MALDI-TOF MS**—Immunoprecipitation followed by MALDI-TOF MS analysis was carried out as described previously (19). Briefly, cell lines were grown to confluence in 8-cm dishes. The culture media were replaced with media with or without 20 ng/ml PMA. After 6 h, the media were collected and immunoprecipitated by incubation for 8 h at 4°C with antibody 6521. Following washing, immunoprecipitated peptides were eluted and analyzed by MALDI-TOF MS. Molecular masses and heights of the MS peaks were calibrated with angiotensin (Sigma), bovine insulin  $\beta$ -chain (Sigma), or both.

## RESULTS

**Notch-1 Peptides Are Secreted Extracellularly during Notch Signaling**—Notch ligand binding to Notch receptors results in sequential proteolysis of the receptor, and PS-dependent intramembrane proteolysis at the interface between the membrane and cytosol (S3) liberates NICD that modifies the transcription of target genes (1) (Fig. 1A). Although it was shown that degradation of Notch-1 transmembrane domain requires additional proteolysis near the middle of the transmembrane domain (S4, dual cleavage) (19), secretion of extracellular small peptides (Notch-1  $A\beta$ -like peptide;  $N\beta$ ) during Notch signaling has not been determined (Fig. 1A). Therefore, we first examined whether sequential endoproteolysis of Notch receptors induced upon binding of Notch ligands (1) results in the secretion of Notch peptides. The full-length Notch-1 receptor does not undergo sequential endoproteolysis in the absence of ligand binding, because the S2 cleavage site is masked in the Notch-1 heterodimer formed by S1-cleaved Notch-1 fragments (1). In contrast, Notch-1 LNR CC > SS (N1CS) (Fig. 1B) inhibits heterodimerization of S1-cleaved Notch-1 (14). Thus, we expect that N1CS shows constitutive consecutive S1, S2, S3, and S4 cleavage of Notch-1 that usually occurs depending on ligand binding (Fig. 1B and supplemental Fig. 1A).

To determine whether Notch-1 peptides are secreted, we metabolically labeled HEK293 cells stably expressing Notch-1 or N1CS with [ $^{35}$ S]methionine and then performed immunoprecipitation using antibody 6521, which binds to an epitope downstream of S2 (Fig. 1B). Most strikingly, autoradiography shows that N1CS-expressing cells secrete Notch-1 peptides of ~3 and 6 kDa, although they were present in different amounts (Fig. 1, C, upper and lower panels, and D). The Notch-1-expressing cells, however, produced only trace amounts of these peptides (Fig. 1C, upper panel). Moreover, addition of PMA to enhance the cleavage at S2 by matrix metalloproteases increased the level of released Notch-1 peptides by  $4.73 \pm 0.01$ -fold (Fig. 1, C and D). On the other hand, addition of  $\gamma$ -secretase inhibitors (L685,458 or DAPT) to inhibit dual-intramembrane proteolysis at S3 and S4 by PS-dependent endoproteolysis greatly reduced the amount of secreted Notch-1 peptide (Fig. 1D and supplemental Fig. 1B). These results indicated that the Notch-1 peptides are secreted in conjunction with the sequential proteolysis of the Notch-1 receptor and that the production of the Notch-1 peptides is associated with the efficiency of cleavage at S2 and S3/S4 by metalloproteases and PS-dependent proteases, respectively.

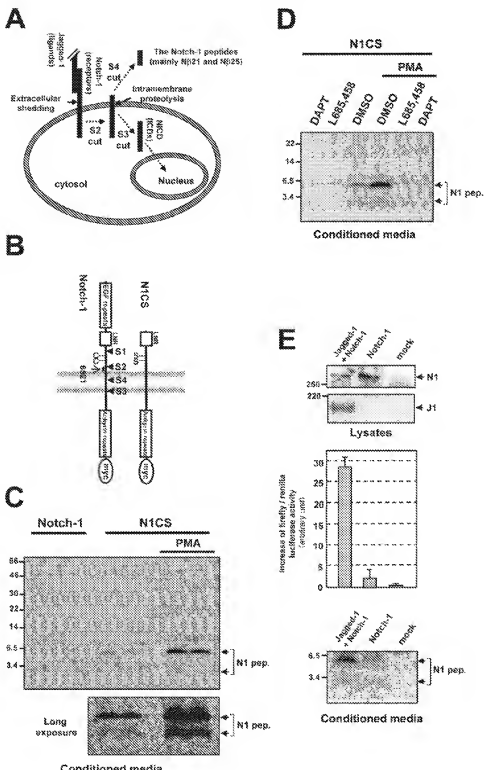
We next investigated whether the Notch-1 peptides are secreted during Notch signaling (Fig. 1E). Instead of N1CS, we used Notch-1 without any extracellular truncation and mutations (Fig. 1B) and observed Notch signaling mediated by Jagged-1 (a Notch ligand). We simultaneously measured the level of Notch signaling and analyzed whether Notch-1 peptides are secreted from cells expressing Jagged-1, Notch-1, or both (Fig. 1E). To determine the level of Notch signaling, we measured luciferase reporter activity in cells expressing *HES-1-luc* (10) (3rd panel in Fig. 1E and supplemental Fig. 2). We also examined the condi-

tions media for the presence of secreted Notch-1 peptides, as described in Fig. 1, C and D. We found that cotransfection with Jagged-1 and Notch-1 greatly increased the reporter activity (3rd panel of Fig. 1E), indicating substantial enhancement of transcription via the *HES-1* promoter. Most surprisingly, the secretion of Notch-1 peptides was also greatly enhanced in cells expressing both Jagged-1 and Notch-1, but it was hardly detectable in cells expressing either Jagged-1 (data not shown) or Notch-1 alone (Fig. 1E, bottom panel). These results indicated that the secretion of the Notch-1 peptides and the activation of Notch signaling are greatly increased when both Notch-1 and its ligand, Jagged-1, are present. In summary, sequential proteolysis of Notch-1 occurs upon Jagged-1 binding, leading to the production of not only NICD, which is released from the membrane to the cytosol (supplemental Fig. 1B), but also novel Notch-1 peptides that are released extracellularly (depicted in Fig. 1A).

**Determination of the Amino Acid Sequences of the Notch-1 Peptides Reveals Secretion of  $N\beta$** —Next, we determined the amino acid sequences of the Notch-1 peptides secreted during the sequential endoproteolytic process of Notch-1 receptor (Fig. 2). The Notch-1 peptide species secreted by N1CS-expressing cells were immunoprecipitated with the 6521 antibodies, and their molecular masses were analyzed by matrix-assisted laser desorption ionization-time of flight (MALDI-TOF) mass spectroscopy (MS) (Fig. 2A). The spectrum of the Notch-1 peptides showed two major peaks with molecular masses of 2306 and 2694 Da. We determined the peptide sequences of these species based on that of the sequence surrounding the epitope for the 6521 antibody. Most strikingly, the Notch-1 peptides were found to be composed of peptides S2 to S4 (Table 1, supplemental Fig. 3, and supplemental Table 1). Finally, amino acid sequences of the Notch-1 peptides were determined by MALDI-TOF/TOF MS analysis (supplemental Fig. 3). Therefore, we found that these Notch-1 peptides correspond to the previously predicted  $N\beta$  (19). We named the shorter (2306 Da) and longer (2694 Da)  $N\beta$  species  $N\beta 21$  and  $N\beta 25$ , respectively, where the number indicates the peptide length (Table 1).

We next synthesized  $N\beta 21$  and  $N\beta 25$  and analyzed them by MALDI-TOF MS. We confirmed that each peptide showed a single peak in the MS spectrum corresponding to the predicted molecular mass (Fig. 2B). We then examined the characteristics of each peptide on Tris-Tricine SDS-PAGE (Fig. 2C). We dissolved these peptides in 1,1,1,3,3,3-hexamethoxy-2-propanol (HFIP) to prevent the formation of artificial oligomers (32) or in Me<sub>2</sub>SO. In both cases, the migration of synthetic  $N\beta 25$  and  $N\beta 21$  approximately corresponded to 3- and 6-kDa bands, respectively (Fig. 2C, left and middle panels). These results showed that, unlike  $N\beta 25$  (or FLAG-tagged  $N\beta$  species (19)),  $N\beta 21$  may form an SDS-stable homodimer. Like  $A\beta$ , we detected extremely low levels of intracellular  $N\beta$  compared with secreted  $N\beta$ , but we did not detect higher molecular weight aggregates of secreted  $N\beta 21$  or  $N\beta 25$  on Tris-Tricine SDS-PAGE (data not shown). Also, the intensity of the ~6-kDa band of a mixture prepared with  $N\beta 21$  and  $N\beta 25$  species was not affected (Fig. 2C, left panel), indicating that the two  $N\beta$  species do not form a heterodimer. Thus,  $N\beta 21$  and  $N\beta 25$  are separated well by SDS-PAGE. Most interestingly, the migrations of secreted (Fig. 2C, right panel) and synthetic  $N\beta$  (Fig. 2C, middle panel) on SDS-PAGE were almost identical. Moreover, upon PS1 L166P mutant expression, the ~3-kDa  $N\beta$  band on SDS-PAGE and the MS peak corresponding to  $N\beta 25$  were predominantly detected (see Fig. 3, A and C). These findings indicate that  $N\beta 21$  and  $N\beta 25$  are the major types of secreted  $N\beta$ . Measurement of the radioactivity of the two bands indicated that ~20% as much  $N\beta 25$  is secreted from cultured cells as  $N\beta 21$  (Fig. 2D). Based on these results, it appears that the secreted  $N\beta$  species correspond to the

**FIGURE 1.** Extracellular release of the Notch-1 peptides by sequential cleavage during Notch signaling. *A*, schematic representation of the Notch-1 peptide ( $N\beta$ ) release during canonical Notch signaling. Cleavage of Notch-1 at S4 results in the extracellular secretion of  $N\beta$  species (see below), whereas cleavage at S5 liberates NICD, which translocates to the nucleus to regulate target gene transcription. *B*, schematic representation of Notch-1 and N1 LNR CC > 55 (N1CS), a peptide derived from Notch-1, S1 to S4 and the gray zone represent the sites of proteolysis and membrane, respectively. The Notch-1 and N1CS constructs both had C-terminal hexameric Myc tags. Note that the N1CS protein lacks the epidermal growth factor repeats present in Notch-1. Also, to avoid the formation of heterodimers following cleavage at S1, the cysteine residues between S1 and S2 were mutated to serine (14). The arrow indicates the recognition site for the 6521 antibody. *C*, immunoprecipitation/autoradiography analysis of Notch-1 peptides in conditioned media from cells treated without or with PMA. Notch-1 or N1CS-expressing cells were labeled by pulse-chase with [ $^{35}$ S]methionine. The Notch-1 peptides in conditioned media were separated by Tricine SDS-PAGE. The lower panel, which shows a longer exposure of the autoradiograph, confirms that without PMA treatment the Notch-1 peptides have two distinct molecular weights. Immunoprecipitation/immunoblotting analysis with a 9E10 antibody revealed that the levels of Notch-1 and N1CS expression were similar in the stably transfected cells (data not shown). *D*, immunoprecipitation/autoradiography analysis of conditioned media from N1CS-expressing cells treated with or without  $\gamma$ -secretase inhibitors. The  $\gamma$ -secretase inhibitors DAPT (1  $\mu$ M) and L655,458 (1  $\mu$ M) inhibited the secretion of the Notch-1 peptides. Similar results were obtained using HeLa cells expressing N1CS (data not shown). DMSO, Me<sub>2</sub>SO. *E*, measurement of Notch signaling and the release of Notch-1 peptides in cells transfected with Jagged-1, Notch-1, or both. HEK293 cells were transiently transfected with the indicated constructs along with HES-1-luc and the pRL-TK dual luciferase reporter assay system. Empty plasmid vector was used as a mock transfection control. The results show cells expressing HES-1-luc. Similar results were observed using cells expressing pGKgfp-Notch-1 (data not shown). *F*, top panel, to confirm the expression of Notch-1, Western blot/immunoblot analysis was carried out using anti-Myc antibody 9E10. *G*, bottom panel, Jagged-1 expression was determined using anti-Jagged-1 antibody H114. *H*, middle panel, assay of Notch downstream signaling. A dual luciferase reporter assay was performed to compare the transcriptional activity of the HES-1 promoter in each condition. HES-1 promoter activity was measured as the relative ratio of firefly and *Renilla* luciferase activities. All values were corrected by the background luciferase activity in endogenous Notch-expressing cells transfected with HES-1-luc and pRL-TK. *I*, bottom panel, conditioned medium from [ $^{35}$ S]methionine-labeled cells was analyzed by immunoprecipitation/autoradiography using antibody 6521.



sequence between S2 and S4 of Notch-1 and that N $\beta$  is made up of two major species, N $\beta$ 21 and N $\beta$ 25, of which the former is predominant in cell culture (Fig. 2*D*).

Several Familial AD-associated *PSI* Mutants Increase the Generation of Elongated N $\beta$  as Well as the Pathological Elongated A $\beta$ —Our results show that intramembrane cleavage of Notch-1 at S4 generates two major N $\beta$  species. We therefore refer to these cleavages as S4-21 and S4-25 for N $\beta$ 21 and N $\beta$ 25, respectively (Fig. 3*D*). S4-25, the minor type

of S4 cleavage, is located four amino acids C-terminal to S4-21, the major S4 cleavage. Like Notch-1,  $\beta$ APP undergoes PS-dependent intramembrane proteolysis near the middle of the transmembrane domain ( $\gamma$ ), resulting in the secretion of A $\beta$ , which accumulates in AD brains (22). Topologically, the  $\gamma$ -cleavage site of  $\beta$ APP corresponds to the S4 cleavage site of Notch-1 (19). Cleavage at  $\gamma$ k2, an alternative form of  $\gamma$ -cleavage, generates A $\beta$ k2, which plays a causative role in the pathology of AD; therefore, understanding the mechanism of PS-de-

## Secretion of N $\beta$ during Notch Signaling

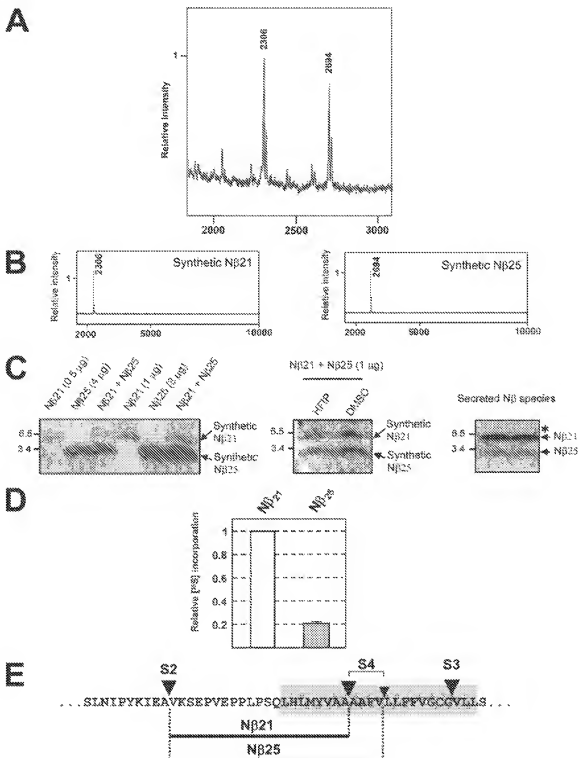


**FIGURE 2.** Identification and characterization of secreted N $\beta$  species. *A*, determination of the molecular masses of the secreted Notch-1 peptides. N1CS-expressing cells were treated with 20 ng/ml PMA for 3 h, and the conditioned medium was analyzed by immunoprecipitation/MS analysis using antibody 6521. Shown is a representative MS spectrum. The MS spectrum was nearly identical for conditioned medium from cells transiently coexpressing Jagged-1 and Notch-1, although the peak heights were lower (data not shown). *B*, MALDI-TOF MS spectra of the synthetic N $\beta$ 21 and N $\beta$ 25. Although the synthetic N $\beta$ 21 appears as an ~6-kDa band on electrophoresis and may form an SDS-stabilized dimer (C), both the synthetic N $\beta$ 21 and N $\beta$ 25 are detected as single peaks in the MS analysis corresponding to monomeric forms. This shows that the mobility of N $\beta$ 21 on SDS-PAGE is lower than predicted. The molecular masses were determined by MALDI-TOF MS. *C*, SDS-PAGE analysis of the synthetic N $\beta$ 21, synthetic N $\beta$ 25, and secreted Notch-1 peptides. Left panel, the synthetic N $\beta$ 21 and N $\beta$ 25 are separated by Tris-Tricine SDS-PAGE. Right panel, zymogram analysis of the synthetic N $\beta$ 21 and secreted Notch-1 peptides. Center panel, the synthetic N $\beta$ 21 and N $\beta$ 25 are dissolved in HRP/PV MeSO and separated by Tris-Tricine SDS-PAGE. Because of the hydrophobic nature of the synthetic N $\beta$ 21 and N $\beta$ 25, they do not dissolve in HRP/PV MeSO and contain a hydrophobic transmembrane domain sequence; therefore, we suspended the synthetic N $\beta$  in HRP to completely solubilize the peptides. We then examined whether the mobility on electrophoresis of the N $\beta$  species was affected by the solvents. We were not able to detect the ~3-kDa monomeric N $\beta$ 21 band by electrophoresis. Note that similar intensities were observed for the N $\beta$ 21 or N $\beta$ 25 bands when equal amounts of the synthetic peptides were applied to the gel, indicating that the S9 antibody has similar affinities for the N $\beta$ 21 and N $\beta$ 25. *D*, right panel, N $\beta$  peptides in conditioned media from [ $^{35}$ S]methionine-labeled cells were separated by Tris-Tricine SDS-PAGE. The asterisk indicates a faint ~8-kDa band that was occasionally observed only in conditioned medium. The radioactivity of this band accounts for less than 5% of the total for all N $\beta$  species, indicating a

**TABLE 1**  
**Major molecular species of the Notch-1 peptides in conditioned media**

M <sub>r</sub> (observed)	Peptide	Sequence	M <sub>r</sub> (calculated)
2306	N $\beta$ 21	VKSKEPVPEPLPSQLHLMLVAA	2306
2694	N $\beta$ 25	VKSKEPVPEPLPSQLHLMLVAAA	2694

pendent intramembrane endoproteolysis is an important issue in AD research (22).

To address the mechanism of cleavage at S4, which results in the production of N $\beta$ , we next tested whether the precision of this cleavage varies simultaneously with the precision of  $\gamma$ -cleavage in  $\beta$ APP. Most familial AD-associated PS mutants increase the relative level of secreted A $\beta$ 42 peptides, although the magnitude of the increase varies between mutants (22). We first tested whether the precision of S4 cleavage was affected by several types of PS mutants. Cells stably expressing the substrates sw mutant  $\beta$ APP and N1CS, as well as WT or mutant forms PS1 (Fig. 3), were metabolically labeled with [<sup>35</sup>S]methionine. Secreted N $\beta$  or A $\beta$  species were immunoprecipitated and separated by Tris-Tricine or Tris-Bicin (38) SDS-PAGE, respectively (Fig. 3A). To measure the efficiency of N $\beta$ 25 generation (S4-25 cleavage), we calculated the relative ratio of radioactivity of the N $\beta$ 25 band compared with the total for N $\beta$  bands (including N $\beta$ 25; Fig. 3B). Using the same samples, we also determined the efficiency of A $\beta$ 42 generation ( $\gamma$ 42 cleavage). We found that the conditioned medium from cells expressing the PS1 L166P mutant, which has been reported to strongly promote A $\beta$ 42 generation (40), had much higher levels of A $\beta$ 42 than the medium from cells expressing WT PS1 (Fig. 3, A, lower panel and B). Most strikingly, SDS-PAGE analysis of the N $\beta$  species in the same media (Fig. 3A, upper panel) showed that the major species was  $\sim$ 3 kDa (N $\beta$ 25) and the minor species was  $\sim$ 6 kDa (N $\beta$ 21), which is opposite the relative amounts in cells expressing WT PS1. MS analysis of the media of PS1 L166P expressing cells confirmed that the major secreted N $\beta$  species are N $\beta$ 21 and N $\beta$ 25 with minor other species (Fig. 3C).

Therefore, PS1 L166P greatly enhanced not only the production of the long and pathological form of A $\beta$  (A $\beta$ 42), but also the production of the longer form of N $\beta$  (N $\beta$ 25) (Fig. 3, A and C). Likewise, the relative ratio of N $\beta$ 25 secreted from cells expressing PS1 L286V, PS1 D9, and other tested mutants except for C92S (39) increased compared with cells expressing WT PS1 (Fig. 3B and data not shown). We therefore suggest that S4-21 and S4-25 cleavage of Notch-1 are  $\gamma$ 40- and  $\gamma$ 42-like cleavage of  $\beta$ APP, respectively (Fig. 3D).

*Modifications of Intramembrane Proteolysis in an Endogenous WTPS Background Have Similar Effects on the Precision of S4 and  $\gamma$  Cleavages*—Recent findings suggest that the relative level of A $\beta$ 42 can be changed without mutations in PS or  $\beta$ APP by using certain chemicals (29, 30). A subset of NSAIDs either increases (29) or decreases (30) the level of A $\beta$ 42 generation. Therefore, we finally examined whether, in an endogenous PS background, chemicals can cause parallel changes in the relative levels of N $\beta$ 25 and A $\beta$ 42. To lower A $\beta$ 42, we used sulindac sulfide (100  $\mu$ M), indometacin (100  $\mu$ M) (29), and a newly developed compound, 3,5-bis(4-nitrophenyl)-benzoic acid, which is called compound W (CW) (100  $\mu$ M). CW was the most effective of  $\sim$ 100 tested compounds identified in a computer-based structural similarity search

for NSAIDs that affect the production of A $\beta$ 42. The cells were treated with the compounds and then subjected to metabolic labeling with [<sup>35</sup>S]methionine. The levels of A $\beta$ /N $\beta$  species were measured as described in Fig. 3. Remarkably, we found that the tested compounds all decreased the relative level of released N $\beta$ 25 as well as A $\beta$ 42 (Fig. 4, A, left panels, and B). Of these compounds, the most effective, CW, caused a drastic decrease in the level of secreted N $\beta$ 25 (Fig. 4A, upper left panel) and A $\beta$ 42 species (Fig. 4A, middle and lower left panels). Next, we examined the effects of S2472 (20  $\mu$ M), fenofibrate (100  $\mu$ M), farnesyl pyrophosphate ammonium salt (10  $\mu$ M), and geranylgeranyl pyrophosphate ammonium salt (10  $\mu$ M), which are compounds that raise the level of A $\beta$ 42 (30). As expected, these compounds all increased the relative level of A $\beta$ 42 (Fig. 4, A, right panels, and B). Notably, in all the cases analyzed, the relative level of N $\beta$ 25 generation was simultaneously increased (Fig. 4B). Naproxen did not modify the relative level of A $\beta$ 42 (29) or N $\beta$ 25 (Fig. 4, B and C). A plot of the ratio of N $\beta$ 25 to total N $\beta$  versus the ratio of A $\beta$ 42 to total A $\beta$  (Fig. 4C) showed a strong linear correlation ( $R^2 = 0.98$ ) between the changes in the relative levels of N $\beta$ 25 and A $\beta$ 42. Moreover, the total level of A $\beta$  and N $\beta$  was not changed by any of the compounds, suggesting that they affect the selectivity but not the activity of cleavage (Fig. 4A). These results indicate that, even in cells expressing endogenous PS, the chemicals caused a concomitant change in the relative levels of N $\beta$ 25 and A $\beta$ 42.

## DISCUSSION

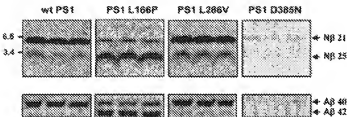
In this study, we showed that N $\beta$  species are secreted from cells as a result of sequential Notch-1 proteolysis during Notch signaling. Upon ligand binding, these peptides are likely generated by PS-dependent intramembrane endoproteolysis at S4 after shedding of the extracellular domain (cleavage at S2). Similarly, AD-associated A $\beta$  species are produced by the PS-dependent proteolysis of  $\beta$ APP (41, 42). Based on these findings, we suspect that cleavage at the middle of the transmembrane domain and extracellular secretion of A $\beta$ -like peptides (e.g. N $\beta$ ) are a common occurrence in PS-dependent intramembrane proteolysis, even though secretion of such peptides is not included in the current model of RIP signaling.

The human *Notch-1* homologue, *TAN-1*, was isolated as a protein that binds to a mutant  $\beta$  T cell receptor gene formed by chromosomal translocation in human T lymphoblastic leukemia, suggesting that *Notch-1* is involved in tumorigenesis as well as development (8). Moreover, more than 50% of human T lymphoblastic leukemia, including tumors from all major molecular oncogenic subtypes, have activating mutations in Notch-1 (9). Thus, further studies are necessary to determine whether secreted N $\beta$  participates in tumorigenesis or has any other physiological functions in development. In addition, it will be interesting to investigate whether the amount of secreted N $\beta$  reflects the level of Notch signaling so that N $\beta$  might be used as a tumor marker.

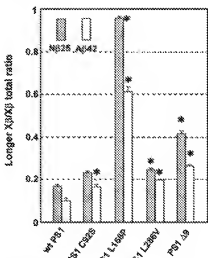
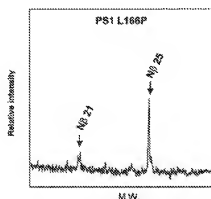
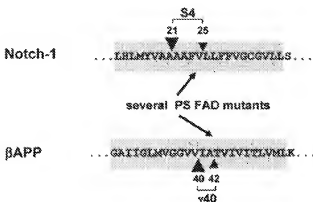
In this study, N $\beta$  consisted mainly of a major N $\beta$ 21 species and a minor N $\beta$ 25 species, indicating that S4 cleavage occurs primarily at two sites, S4-21 and S4-25, in the middle of the Notch-1 transmembrane domain. This confirms that dual-intramembrane proteolysis occurs at S3 and S4 upon degradation of the transmembrane domain of Notch-1 (19). Moreover, the diversity in the sites of cleavage in the middle of the transmembrane domain is reminiscent of the mechanism producing A $\beta$ 42, a peptide that plays a causative role in AD (22). Therefore, we

very minor species of N $\beta$  may be released in addition to N $\beta$ 21 and N $\beta$ 25. D, the relative ratio of N $\beta$ 25 to that of N $\beta$ 21 in the conditioned media of cells stably expressing N1CS. Cells were labeled with [<sup>35</sup>S]methionine, and radiolabeled N $\beta$  peptides in the conditioned medium were separated by Tris-Tricine SDS-PAGE. The radioactivity incorporated into each band was measured by fluorography using a STORM 820 (Amersham Biosciences). The radioactivity was normalized by that of the N $\beta$ 21 band. The bars represent the means of three independent measurements, and the error bars indicate the S.D. E, schematic representation of two different N $\beta$  species and the S2, S3, S4 in Notch-1. The gray box indicates the putative transmembrane domain of murine Notch-1.



**A**

**FIGURE 3.** The effects of PS1 mutants on the secretion of the longer N $\beta$ . *A*, N $\beta$  and A $\beta$  secreted from cells expressing PS1 mutants. *Upper panels*, N $\beta$  species were analyzed as described in Figs. 1 and 2. *Lower panels*, A $\beta$  was immunoprecipitated with antibody 4G8 and separated by Tris-Bicinchoninic acid SDS-PAGE. Note that N $\beta$  and A $\beta$  are hardly detectable in cells stably expressing PS1 D385N, which is dominant negative for PS-dependent protease activity. *B*, the relative ratio of longer X $\beta$  [N $\beta$ 25 and A $\beta$ 42] secreted by cells expressing familial AD-associated PS mutants. Three independent experiments were carried out with each of two different stable cell lines. Asterisks indicate that the ratio of longer X $\beta$  was statistically higher than that in WT PS1-expressing cells ( $p < 0.001$  by Student's *t*-test). Similar results were obtained in CHO cells expressing familial AD-associated PS1 mutants (36). *C*, MS spectrum of N $\beta$  species secreted from cells expressing the PS1 L166P mutant. The N $\beta$ 25 peak was much higher than the N $\beta$ 21 peak comparing the case of WT PS1 (see Fig. 2*A*). Note that the N $\beta$  peptides secreted by the cells are mainly N $\beta$ 25 and N $\beta$ 21. *D*, schematic representation of the sites cleaved in Notch-1 and  $\beta$ APP by PS-dependent intramembrane proteolysis during the generation of X $\beta$  species. Gray boxes indicate the putative transmembrane domain in Notch-1 and  $\beta$ APP. The arrowheads show the S4 and  $\gamma$ -cleavage sites. Arrows show the sites where the efficiency of cleavage is affected by tested familial AD-associated PS mutants.

**B****C****D**

tested whether the relationship between N $\beta$ 21 and N $\beta$ 25 was similar to that between A $\beta$ 40 and A $\beta$ 42. Most familial AD-associated PS mutants increase the generation of A $\beta$ 42 (22). Thus, we examined whether the PS mutants result in an extended C terminus in N $\beta$ . We found that, except for the PS1 C92S mutant, the tested PS mutants increased the relative amount of N $\beta$ 25. One possible reason for this anomaly is that the mechanism by which the PS1 C92S mutant enhances A $\beta$ 42 generation affects Notch-1 processing differently. Another possibility is that the mutant is simply not strong enough to significantly increase the production of N $\beta$ 25. Moreover, the PS1 L166P mutants that greatly increased the level of A $\beta$ 42 also greatly increased the level of N $\beta$ 25.

Therefore, in many cases, PS1 mutants that affect the precision of intramembrane proteolysis of  $\beta$ APP have similar effects on Notch-1 cleavage.

A $\beta$ 42 accounts for ~10% of the total A $\beta$  in cells expressing endogenous PS (22). Recently, several NSAIDs were found to either increase or decrease the relative production of A $\beta$ 42 (29, 30). This is extremely important because it shows that, as in sporadic AD, the precision of  $\gamma$ -cleavage can change without mutation in either in the substrate ( $\beta$ APP) or the key enzyme component (PS). This prompted us to investigate whether such compounds also affect the C terminus of N $\beta$ . Because NSAIDs affect the precision of  $\gamma$ -cleavage independently of its

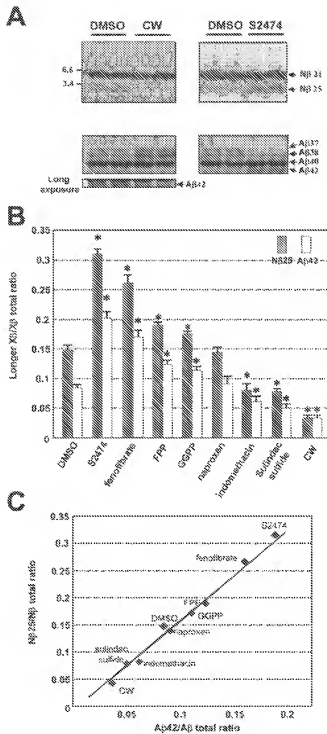


**FIGURE 4.** Effects of compounds that modify the generation of A $\beta$ 42 on the secretion of longer N $\beta$ 25. **A**, Effect of various compounds on the secretion of N $\beta$  and A $\beta$  species from cells expressing  $\beta$ APP sw and NTCS. Note that the decrease in the level of A $\beta$ 42 occurred concomitantly with an increase in the level of A $\beta$ 37/38 generation. Likewise, an increase in the level of A $\beta$ 42 was accompanied by a decrease in the level of A $\beta$ 37/38 generation. DMSO, Me<sub>2</sub>SO, B, the relative ratio of longer X/B (N $\beta$ 25 and A $\beta$ 42) secreted from endogenous PS-expressing cells treated with various compounds. Asterisks indicate that the relative ratio was statistically different from the Me<sub>2</sub>SO control ( $p < 0.01$  by Student's *t* test). C, a scatter plot of the relative ratio of N $\beta$ 25 versus the relative ratio of A $\beta$ 42. The same experiments as in panel B were independently repeated.

anti-inflammatory function (43), we performed a structure similarity search of A $\beta$ 42-lowering NSAIDs, and we identified CW as being the most effective of ~100 compounds. Strikingly, all of the tested compounds that affected the level of A $\beta$ 42 caused parallel changes in the

generation of N $\beta$ 25. These results suggest that N $\beta$ 25 is the molecular species that corresponds to A $\beta$ 42 and that the PS-dependent protease generates longer N $\beta$  and longer A $\beta$  by a common mechanism.

Although increased production of A $\beta$ 42 is thought to cause the pathogenesis of most forms of familial AD, abnormalities in A $\beta$  metabolism rather than increased A $\beta$ 42 generation are thought to be central to the pathogenesis of sporadic AD (44). Notably, the level of A $\beta$  peptides, especially A $\beta$ 42, in peripheral blood and cerebrospinal fluid do not correlate with their levels in the central nervous system because they tend to aggregate. Therefore, whether A $\beta$ 42 generation changes in sporadic AD remains unknown. In this study, we showed that longer A $\beta$ -like peptide species (N $\beta$ 25) and A $\beta$  (A $\beta$ 42) are secreted concomitantly, which suggests that elongated A $\beta$ -like peptides that do not aggregate could be used as surrogate markers for A $\beta$ 42 production.

In this study, we found that S4 and  $\gamma$ -cleavages, which occur in the middle of the transmembrane domain, have nearly identical characteristics. Also, S3 and  $\epsilon$  cleavages, which occur near the cytosol-membrane interface, are very similar (40, 45).<sup>4</sup> Thus, PS-dependent intramembrane proteolysis may be mediated by a common mechanism in Notch-1 and  $\beta$ APP. However, the processes mediating cleavage at  $\epsilon$  and S3 seem to be distinct from that mediating  $\gamma$ -cleavage (40). Therefore, PS-dependent intramembrane proteolysis in the middle of the transmembrane domain (S4 and  $\gamma$ ) and at the membrane-cytosol interface ( $\epsilon$  and S3) appears to be mediated by distinct mechanisms.

The effect of NSAIDs on the precision of PS-dependent intramembrane proteolysis was thought to be  $\beta$ APP-specific because the compounds affected precision of  $\gamma$ -cleavage but not the level of S3 cleavage (which generates NICD) (29). Our results, however, suggest that the effects of the compounds are not substrate-specific but may affect S4- and  $\gamma$ -like cleavages that occur near the middle of the transmembrane domains.

Comparison of the processes and precision of S4 and  $\gamma$  cleavage should help clarify how A $\beta$  and A $\beta$ 42, essential molecules in AD pathology, are generated. The  $\beta$ APP  $\gamma$ -cleavage shares the following characteristics with Notch-1 S4 cleavage. (i) Both of the cleavages occur near the middle of the transmembrane domain (19). (ii) Both have alternative cleavage sites (see Fig. 3D). (iii) Several familial AD-associated PS mutations enhance the cleavage efficiencies at minor C-terminal sites of both peptides (S4-25 and  $\gamma$ 12). (iv) Several compounds simultaneously change both S4-25 and  $\gamma$ 12 cleavage efficiencies. Although the amino acid sequences of the transmembrane domains of Notch-1 and  $\beta$ APP are quite different, they are thought to both contain  $\alpha$ -helical structures (see Fig. 3D). Therefore, the common aspects of S4 and  $\gamma$ -cleavage do not appear to be due to similarities in the primary structure of the substrate (transmembrane domains of Notch-1 and  $\beta$ APP) but rather similarities in the secondary structures or higher structures of the enzyme-substrate complex.

Although there are significant similarities in the two cleavages, there are also some minor differences as follows. (i) The major  $\gamma$ -site is almost in the center of the transmembrane domain of  $\beta$ APP, whereas the corresponding site in Notch-1, S4-21, is located slightly toward the extracellular side in the transmembrane domain (Fig. 3D). (ii) The distance between the major  $\gamma$ 10 and the minor  $\gamma$ 12 site is two amino acids, whereas the distance between S4-21 and S4-25 is four amino acids (Figs. 2E and 3D). (iii) The cleavage efficiency at  $\gamma$ 12 is ~10%, whereas that of S4-25 is ~20% (Fig. 2D). These distinct properties are likely to be at least partly because of differences in the primary structures of the substrates. Comparison of the characteristics of S4 and  $\gamma$ -cleavage should help

<sup>4</sup>A. Fukumori, S. Tagami, and M. Okochi, submitted for publication.



clarify the process of A $\beta$ 42 generation; specifically, it appears that the peptide secondary or the higher structure of the enzyme-substrate complex is involved in the efficiency of A $\beta$ 42 generation, whereas the primary structure of the substrate transmembrane domain appears to determine the site of the minor cleavage.

When cleaved by PS-dependent intramembrane proteolysis, the  $\beta$ APP transmembrane domain is thought to maintain an  $\alpha$ -helical conformation (46). In this case, the pathological  $\gamma$ 42 cleavage would occur in the opposite orientation as the major  $\gamma$ 40 cleavage. In contrast, although the corresponding S4-25 site is located more toward the cytosolic side of the transmembrane domain, it is in nearly the same orientation at the S4-21 site. Thus, assuming  $\alpha$ -helical structures of the substrate, cleavage at S4-25 and  $\gamma$ 42 would be expected to occur by different mechanisms. Because there are so many similarities between the two, we propose that until the cleavage, perhaps in the enzyme-substrate complex, the secondary structures of the substrate transmembrane domains change so that they are no longer  $\alpha$ -helices.

In this study we showed that N $\beta$  species (mainly N $\beta$ 21 and N $\beta$ 25) are released extracellularly during the process of Notch signaling. The N $\beta$  species had identical N termini but different C termini because of diversity in the site of S4 cleavage. Furthermore, the characteristics of the C-terminal elongation of N $\beta$  and A $\beta$  were almost identical. Because many membrane-bound receptors undergo PS-dependent intramembrane proteolysis, we propose that secretion of A $\beta$ -like peptides such as N $\beta$  may be a common phenomenon. This should open the door to a search for the best A $\beta$ -like peptide to serve as a surrogate marker for AD-associated production of A $\beta$ 42.

**Acknowledgments—**We thank Dr. Rafael Kopan, Dr. Jeffrey S. Nye, Dr. Alain Israel, and Dr. George W. Borkmann for providing cDNAs and constructs; Dr. Dennis J. Selkoe for providing cell lines; Dr. Kazuya Nakao, Dr. Yasuo Ihara, Dr. Makoto Morishima, and Dr. Taisuke Tomita for helpful suggestions.

## REFERENCES

1. Selkoe, D., and Kopan, R. (2003) *Annu. Rev. Neurosci.* **26**, 565–597
2. Mumm, J. S., and Kopan, R. (2000) *Dev. Biol.* **215**, 151–165
3. Brown, M. S., Ye, J., Rawson, R. B., and Goldstein, J. L. (2000) *Cell* **100**, 391–398
4. Wolfe, M. S., and Kopan, R. (2004) *Science* **305**, 1119–1123
5. Le Borgne, R., Bardin, A., and Schweigert, F. (2005) *Development (Camb)* **132**, 1751–1762
6. Schweigert, F. (2004) *Curr. Biol.* **14**, R129–R138
7. Artavanis-Tsakonas, S., Matsuno, K., and Fortini, M. E. (1995) *Science* **268**, 225–232
8. Ellisen, L. W., Bird, J., West, D. C., Soreng, A. L., Reynolds, T. C., Smith, S. D., and Sklar, J. (1991) *Cell* **66**, 649–661
9. Weng, A. P., Ferrando, A. A., Lee, W., Morris, J. P. T., Silverman, L. B., Sanchez-Irizarry, C., Blacklow, S. C., Look, A. T., and Aster, J. C. (2004) *Science* **306**, 269–271
10. Jariwalla, S., Brou, C., Logeat, F., Schroeter, E. H., Kopan, R., and Israel, A. (1995) *Nature* **377**, 355–358
11. Minoguchi, S., Taniguchi, Y., Kato, H., Okazaki, T., Strobl, L. J., Zimber-Strobl, U., Borkmann, G. W., and Honjo, T. (1997) *Mol. Cell. Biol.* **17**, 2679–2687
12. Blaumüller, C. M., Qi, H., Zagouras, P., and Artavanis-Tsakonas, S. (1997) *Cell* **90**, 281–291
13. Logeat, F., Bessia, C., Brou, C., LeBall, O., Jariwalla, S., Seidah, N. G., and Israel, A. (1998) *Proc. Natl. Acad. Sci. U. S. A.* **95**, 8108–8112
14. Mumm, J. S., Schroeter, E. H., Saxena, M. T., Griesemer, A., Tian, X., Pan, D. J., Ray, W. J., and Kopan, R. (2000) *Mol. Cell* **5**, 197–206
15. Brou, C., Logeat, F., Gupta, N., Bessia, C., LeBall, O., Doedens, J. R., Cumano, A., Roux, P., Black, R. A., and Israel, A. (2000) *Mol. Cell. Genes Dev.* **5**, 207–216
16. Lieber, T., Kidd, S., and Young, M. W. (2002) *Genes Dev.* **16**, 209–221
17. Schroeter, E. H., Kissling, J. A., and Kopan, R. (1998) *Nature* **393**, 382–386
18. Drost, S., Annaert, W., Cupers, P., Safig, P., Craessaerts, K., Mumm, J. S., Schroeter, E. H., Schrijvers, V., Wolfe, M. S., Ray, W. J., Goate, A., and Kopan, R. (1999) *Nature* **398**, 518–522
19. Okochi, M., Steiner, H., Fukumori, A., Tanik, H., Tomita, T., Tanaka, T., Iwatsubo, T., Kudo, T., Takeda, M., and Haass, C. (2002) *EMBO J.* **21**, 5408–5416
20. Zhang, J., Ye, W., Wang, R., Wolfe, M. S., Greenberg, B. D., and Selkoe, D. J. (2002) *J. Biol. Chem.* **277**, 15069–15075
21. Haass, C., and Steiner, H. (2002) *Trends Cell Biol.* **12**, 556–562
22. Selkoe, D. J. (2001) *Physiol. Rev.* **81**, 741–766
23. Cao, X., and Sudhoff, T. C. (2001) *Science* **293**, 115–120
24. Pardossi-Piquard, R., Petit, A., Kawarai, T., Sunach, C., Alves da Costa, C., Vincent, B., Ring, S., D'Adamo, L., Shen, J., Müller, U., St. George-Hyslop, P., and Checler, F. (2005) *Neuron* **46**, 541–554
25. Sato, T., Dohmoto, N., Qu, Y., Kakuda, N., Misison, H., Mitsumori, R., Maruyama, H., Koo, E. H., Haass, C., Takio, K., Morishima-Kawashima, M., Ishura, S., and Ihara, Y. (2003) *J. Biol. Chem.* **278**, 24294–24301
26. Xia, W., and Wolfe, M. S. (2003) *J. Cell Sci.* **116**, 2839–2844
27. Koo, E. H., and Kopan, R. (2004) *Nat. Med.* **10**, S26–S33
28. Lammich, S., Okochi, M., Takeda, M., Kaether, C., Capell, A., Zimmer, A. K., Edsbaer, D., Walter, J., Steiner, H., and Haass, C. (2002) *J. Biol. Chem.* **277**, 44754–44759
29. Weggen, S., Ericksen, J. L., Das, P., Sagi, S. A., Wang, R., Pietrzik, C. U., Findlay, K. A., Smith, T. E., Murphy, M. P., Butler, T., Kang, D. E., Marquez, R., Sterling, N., Golde, T. E., and Koo, E. H. (2001) *Nature* **414**, 212–216
30. Kukar, T., Murphy, M. P., Ericksen, J. L., Sagi, S. A., Weggen, S., Smith, T. E., Ladd, T., Khan, M. A., Karch, R., Beard, J., Dodson, M., Merit, S., Ozols, V. V., Anastassiadis, P. Z., Das, P., Faquin, A., Koo, E. H., and Golde, T. E. (2005) *Nat. Med.* **11**, 545–550
31. Okochi, M., Ishii, K., Usami, M., Sahara, N., Kametani, F., Tanaka, K., Fraser, P. E., Ikeda, M., Saunders, A. M., Hendriks, L., Shoji, S. I., Lee, L. M., Martin, J. J., Van Broeckhoven, C., St. George-Hyslop, P. H., Roses, A. D., and Mori, H. (1997) *FEBS Lett.* **418**, 162–166
32. Yoshida, T., Chu, D. H., Akagi, T., Tanaka, N., and Takashima, A. (2003) *J. Biol. Chem.* **278**, 23648–23655
33. Lindsell, C. E., Shaver, C. J., Boulter, J., and Weinmaster, G. (1995) *Cell* **80**, 909–917
34. Nye, J. S., Kopan, R., and Axel, R. (1994) *Development (Camb)* **120**, 2421–2430
35. Steiner, H., Romig, H., Grin, M. G., Philipp, U., Pesold, B., Citron, M., Baumeister, R., and Haass, C. (1999) *J. Biol. Chem.* **274**, 7615–7618
36. Xia, W., Zhang, J., Khokhlova, D., Citron, M., Podlinsky, M. B., Teplow, D. B., Haass, C., Seubert, P., Koo, E. H., and Selkoe, D. J. (1997) *J. Biol. Chem.* **272**, 7977–7982
37. Okochi, M., Walter, J., Kojima, A., Nakajo, S., Baba, M., Iwatsubo, T., Meijer, L., Kahle, P. J., and Haass, C. (2000) *J. Biol. Chem.* **275**, 390–397
38. Wülfing, J., Smirnov, A., Schnierlein, B., Kelemen, G., Matthes, U., Klafki, H. W., Staufenbiel, M., Huther, G., Rutherford, E., and Komhuber, J. (1997) *Electrophoresis* **18**, 527–532
39. Okochi, M., Elmer, S., Bottcher, A., Baumeister, R., Romig, H., Walter, J., Capell, A., Steiner, H., and Haass, C. (2000) *J. Biol. Chem.* **275**, 40925–40930
40. Moehlmann, T., Winkler, E., Xia, X., Edsauer, D., Murrell, J., Capell, A., Kaether, C., Zheng, H., Ghetti, B., Haass, C., and Steiner, H. (2002) *Proc. Natl. Acad. Sci. U. S. A.* **99**, 8025–8030
41. De Strooper, B., Saftig, P., Craessaerts, K., Vanderstichele, H., Guhde, G., Annaert, W., Von Figura, K., and Van Leuven, F. (1998) *Nature* **391**, 387–390
42. Wolfe, M. S., Xia, W., Ostaszewski, B. L., Diehl, T. S., Kimberly, W. T., and Selkoe, D. J. (1999) *Nature* **398**, 513–517
43. Sagi, S. A., Weggen, S., Ericksen, J., Golde, T. E., and Koo, E. H. (2003) *J. Biol. Chem.* **278**, 31825–31830
44. Selkoe, D. J., and Schenk, D. (2003) *Annu. Rev. Pharmacol. Toxicol.* **43**, 545–584
45. Chen, F., Gu, Y., Hasegawa, H., Ruan, X., Aravaka, S., Fraser, P., Westaway, D., Mount, H., and St. George-Hyslop, P. (2002) *J. Biol. Chem.* **277**, 36521–36526
46. Lichtenhauer, S. F., Wang, R., Grimm, H., Uljon, S. N., Masters, C. L., and Beyreuther, K. (1999) *Proc. Natl. Acad. Sci. U. S. A.* **96**, 3053–3058

